

# DEEPLY-VIRTUAL COMPTON SCATTERING

Xiangdong Ji

Department of Physics

University of Maryland

College Park, Maryland 20742

and

Center for Theoretical Physics

Laboratory for Nuclear Science

and Department of Physics

Massachusetts Institute of Technology

Cambridge, Massachusetts 02139

and

Institute for Nuclear Theory

University of Washington

Seattle, Washington 98195

(U. of M D PP # 97-026    MIT-CTP-2568    September 1996)

## Abstract

We study in QCD the physics of deeply-virtual Compton scattering (DVCS) — the virtual Compton process in the large  $s$  and small  $t$  kinematic region. We show that DVCS can probe a new type of off-forward parton distributions. We derive an Altarelli-Parisi type of evolution equations for these distributions. We also derive their sum rules in terms of nucleon form factors of the twist-two quark and gluon operators. In particular, we find that the second sum rule is related to fractions of the nucleon spin carried separately by quarks and gluons. We estimate the cross section for DVCS and compare it with the accompanying Bethe-Heitler process at CEBAF and HERMES kinematics.

Typeset using REVTeX

---

This work is supported in part by funds provided by the U.S. Department of Energy (D.O.E.) under cooperative agreements # DF-FC 02-94ER 40818 and # D O E-FG 02-93ER -40762.

## I. INTRODUCTION

The Compton process, which refers to elastic scattering of a photon off a charged object, has played an important role in the history of Quantum Electrodynamics: It provided one of the early evidences that the electromagnetic wave is quantized, and hence has the nature of particles [1]. The role of the Compton process in studying the structure of hadrons has been explored since 50's, when Low's low-energy theorems [2], analogous to the well-known Thomson cross section, are derived. Those theorems assert, for instance, that at sufficiently low energy the spin-dependent part of the Compton amplitude is determined by the anomalous magnetic moment of a composite system. Going to higher-order terms in the low-energy expansion, one finds the electric and magnetic polarizabilities [3]. In recent years, experimental and theoretical works in measuring and understanding the polarizabilities of the nucleon and pion have flourished [4].

Generally speaking, however, the Compton process on a composite system is quite complicated. When a point-like constituent absorbs an incoming photon, the system becomes excited. As it propagates in time, the system eventually emits a photon and comes back to the ground state. Quantum-mechanical propagation of a composite system is difficult to handle theoretically, except in special kinematic regions. The low-energy theorems exist for the nucleon Compton scattering because the intermediate propagation at low energy is dominated by the nucleon itself [2]. Another kinematic region known to have simple scattering mechanism is where the  $t$ -channel momentum transfer is large, i.e., the nucleon has a large recoil [5]. In this case, perturbative Quantum Chromodynamics can be used to understand the intermediate propagation. In fact, according to the so-called the power counting rule [6], the most important intermediate states are those created from three valence quarks through hard-gluon exchanges. Simple as it may be, one still has to compute hundreds of Feynman diagrams to obtain the scattering cross section.

The purpose of this paper is to study the Compton scattering by a virtual photon in a special kinematic limit. Assuming the virtual photon is generated by inelastic lepton scattering, we are interested in the Bjorken limit, i.e., the energy and momentum of the virtual photon going to infinity at the same rate. We shall call the process deeply-virtual Compton scattering (DVCS). As we shall discuss in the next section, the basic mechanism for DVCS is a quark absorbing the virtual photon, immediately radiating a real photon and falling back to the nucleon ground state. Thus the physics of DVCS is quite simple.

Our interest in studying DVCS is generated from the fact that it offers a way to measure the off-forward parton distributions (OFFD), a new type of parton distributions that generalize the usual parton distributions and the nucleon form factors. When taking moments of OFFDs, one gets form factors of the spin- $n$ , twist-two quark and gluon operators. When going to the forward limit, OFFDs become the usual quark and gluon distributions. Because the spin-2, twist-two operators are part of the energy-momentum tensor of QCD and because the form factors of the energy-momentum tensor contain information about the quark and gluon contributions to the nucleon spin, DVCS may provide a novel way to measure the fraction of the nucleon spin carried by the quark orbital angular momentum, a subject of great current interest [8].

The presentation of the paper goes like this. In Section II, we consider DVCS in QCD at the tree level. We identify the off-forward parton distributions from the Compton amplitude

and then study some simple aspects of the distributions, such as sum rules. In Section III, we study the leading-log evolution of the ODFPs. The results are presented in the form of generalized Altarelli-Parisi equations. In sections IV, we work out the cross sections for DVCS and the accompanying Bethe-Heitler process and their interference. To be complete, we consider all cases including unpolarized, double-spin and single-spin processes. Estimates are given at the CEBAF and HERMES kinematics. The final section contains comments and discussions.

A preliminary account of the DVCS process appeared in a Letter published early [7]. Subsequently Radyushkin studied the scaling limit at  $z^2 = 0$  from a different angle [9]. Actually, processes similar to DVCS were first considered by Geyer et. al. in studying the anomalous dimensions of light-ray operators [10], where the "interpolating functions" were introduced. The evolution of these functions is found to interpolate the Brodsky-Lepage and Altarelli-Parisi equations.

## II. DEEPLY-VIRTUAL COMPTON SCATTERING AT LEADING ORDER

This section is devoted to studying the virtual Compton scattering in deep-inelastic kinematics and at the leading order in perturbative QCD. The main result is that DVCS is dominated by single-quark scattering, and therefore the amplitude can be expressed in terms of the  $q$ -forward parton distributions. We also study sum rules of these distributions and show that the second sum rule is related to the total quark (gluon) contribution to the spin of the nucleon.

We picture the virtual Compton scattering in Fig. 1, where a nucleon of momentum  $P$  absorbs a virtual photon of momentum  $q$ , producing an outgoing real photon of momentum  $q^0 = q$  and a recoil nucleon of momentum  $P^0 = P + q$ . We focus on the deeply-virtual kinematic region of  $q$ , namely, the Bjorken limit:  $Q^2 = -q^2 \gg 1$ ,  $P \cdot q \gg 1$ , and  $Q^2 = P \cdot q$  finite. In this region, the quark that absorbs the virtual photon becomes highly virtual and hence propagates perturbatively. The simplest mechanism to form the Compton final state is for the quark to promptly radiate a real photon and fall back to the nucleon ground state. This "hand-bag" subprocess is shown in Fig. 2 (a).

In QCD, more complicated "tree" subprocesses are possible. By tree, we mean perturbative diagrams in which every vertex is next to the nucleon blob. For instance, the highly-virtual quark can interact with gluon fields in the nucleon, as shown in Fig. 2 (b); or it can transfer its virtuality to another quark through one-gluon exchanges, as shown in Fig. 2 (c). A detailed calculation shows that both subprocesses are suppressed by  $1/Q^2$  relative to the hand-bag diagram, except when the polarization of the gluon in Fig. 2 (b) is longitudinal. Fortunately, in the light-cone gauge  $A^+ = 0$ , the longitudinally-polarized gluons do not contribute by definition. Thus in the deeply-virtual limit, the single-quark process indeed dominates the Compton scattering.

Of course, one can decorate the hand-bag with radiative loops, such as those shown in Figs. 2 (d) and 2 (e). Those diagrams in certain kinematic region produce leading-log corrections to the simple hand-bag, as we shall discuss in the next section. In other kinematic regions, they give rise to order- $\alpha_s(Q^2)$  radiative corrections and hence can be ignored in the deeply-virtual limit. One exception is the gluon vertex correction for the real photon in Fig. 2 (e), where as the two quark lines have momenta predominantly parallel to the photon

momentum, the diagram has an infrared divergence reflecting the non-perturbative photon wavefunction. Fortunately, a simple calculation shows that the contribution in this kinematic region is suppressed by  $1=Q^2$  relative to the hand-bag due to the hard-gluon propagator.

Thus, in the remainder of this section we concentrate solely on the dominant subprocess in Fig. 2(a).

According to Feynman rules, the hand-bag diagram corresponds to the Compton amplitude,

$$T = i \int \frac{d^4k}{(2\pi)^4} \text{Tr} f \left[ \frac{i}{\not{k} = + \not{q} + i} + \frac{i}{\not{k} + (1-\alpha)\not{q} = \not{q} + i} \right] M(k)g; \quad (1)$$

where  $\alpha$  and  $\beta$  are the polarization indices of the initial and final photons and  $M(k)$  is a quark density matrix,

$$M(k) = \int e^{ikx} d^4x \not{x} P^0_j(\alpha, \beta) ((1-\alpha)\not{x}) P^0_i; \quad (2)$$

where  $0 < \alpha < 1$  reflects the arbitrariness of the looping momentum  $k$ . To proceed further, it is convenient to define a special system of coordinates. We choose  $q$  and  $P = (P + P^0) = 2$  to be collinear and in the  $z$  direction. Introduce two light-like vectors,  $p = (1; 0; 0; 1)$  and  $n = (1; 0; 0; -1) = (2)$ , with  $p^2 = n^2 = 0$ ,  $p \cdot n = 1$ , and  $\alpha$  arbitrary. We expand other vectors in terms of  $p, n$  and transverse vectors,

$$\begin{aligned} P &= p + (M^2=2)n; \\ q &= \alpha p + (Q^2=2\alpha)n; \\ &= (\alpha p + M^2=2n) + \beta; \\ k &= (k \cdot n)p + (k \cdot p)n + k_\perp; \end{aligned} \quad (3)$$

where  $M^2 = M^2 - 2\alpha Q^2 = 4$  and  $\beta = (P \cdot q + (P \cdot q) + Q^2 M^2) = M^2$ . The variable  $\beta$  is analogous to the Bjorken variable  $x_B$  in deep-inelastic scattering. We neglect components of four vectors which do not produce large scalars in the Bjorken limit. Introducing the factor  $\int d^4x \frac{d}{2} e^{i(x \cdot k + n \cdot x)} = 1$  and integrating over  $k$  and  $x$ , we simplify the Compton amplitude to,

$$\begin{aligned} T(P; q) &= \frac{1}{2} (p \cdot n + p \cdot n \cdot g) \int dx \left[ \frac{1}{x = 2 + i} + \frac{1}{x + = 2 - i} \right] \\ & \quad H(x; \alpha; \beta^2) U(P^0) \not{n} U(P) + E(x; \alpha; \beta^2) U(P^0) \frac{i}{2M} \not{n} U(P) \\ & \quad \frac{i}{2} p \cdot n \int dx \left[ \frac{1}{x = 2 + i} - \frac{1}{x + = 2 - i} \right] \\ & \quad H^*(x; \alpha; \beta^2) U(P^0) \not{5} U(P) + E^*(x; \alpha; \beta^2) \frac{n}{2M} U(P^0) \not{5} U(P); \end{aligned} \quad (4)$$

where we have chosen  $\beta = 1=2$  for symmetrical reason.  $H, H^*, E$  and  $E^*$  are off-forward, twist-two parton distributions defined through the following light-cone correlation functions,



$$J_{QCD} = J_q + J_g ; \quad (8)$$

where

$$\begin{aligned} J_q &= \int d^3x \mathbf{x} \times \mathbf{T}_q \\ &= \int d^3x \left[ \frac{y}{2} \tilde{\psi} + \mathbf{y} \times (\mathbf{iD})^3 \right] ; \\ J_g &= \int d^3x \mathbf{x} \times (\mathbf{E} \times \mathbf{B}) ; \end{aligned} \quad (9)$$

Here  $\mathbf{T}_q$  and  $\mathbf{E} \times \mathbf{B}$  are the quark and gluon momentum densities, respectively.  $\tilde{\psi}$  is the Dirac spin-matrix and  $D$  is the covariant derivative. By an analogy with the magnetic moment, one can get the separate quark and gluon contributions to the nucleon spin if knowing form factors of the momentum density, or equivalently the energy-momentum tensor of QCD, at zero momentum transfer. Using Lorentz covariance and other symmetry principles, one can write down four form-factors separately for quark and gluon parts of the energy-momentum tensor,

$$\begin{aligned} \langle P^0 | \mathbf{T}_{q/g} | P^0 \rangle = U(P^0) [ A_{q/g}(\tau^2) (\mathbf{P} \cdot \mathbf{P}) + B_{q/g}(\tau^2) P^i P^i ] = 2M \\ + C_{q/g}(\tau^2) (\mathbf{P} \cdot \mathbf{g}) = M + C_{q/g}(\tau^2) g^i M^i U(P) ; \end{aligned} \quad (10)$$

where again  $P = (P^+ + P^0)/2$ ,  $\tau^2 = P^+ - P^0$ , and  $U(P)$  is the nucleon spinor. Substituting the above into the nucleon matrix element of  $J_{q/g}$ , one finds fractions of the nucleon spin carried by quarks,  $J_q$ , and gluons,  $J_g$ ,

$$\begin{aligned} J_{q/g} &= \frac{1}{2} [A_{q/g}(0) + B_{q/g}(0)] ; \\ J_q + J_g &= \frac{1}{2} ; \end{aligned} \quad (11)$$

According to the definition, the second moment of off-forward parton distributions yields the form factors of the energy-momentum tensor,

$$\int dx x [H(x; \tau^2) + E(x; \tau^2)] = A(\tau^2) + B(\tau^2) ; \quad (12)$$

where luckily the  $\tau$  dependence, or  $C_q(\tau^2)$  contamination, drops out. Extrapolating the sum rule to  $\tau^2 = 0$ , one gets  $J_{q/g}$ . Note that only in this special application, we are interested in  $\tau^2 \rightarrow 0$  limit. In general discussions of DVCS, such limit is of course not necessary.

By forming still higher moments, one obtains form factors of the twist-two operators of spin greater than 2. In general, there are many form-factors for each of the tensor operators; however, only special combinations of them appear in moments of the ODPDs. The relative weighting of the different form factors is determined by variable  $\tau^2$ .

### III. LEADING-LOG EVOLUTION OF OFF-FORWARD PARTON DISTRIBUTIONS

In this section, we study the leading-log evolution of the off-forward parton distributions. Like the leading-log evolution of the usual parton distributions (Altarelli-Parisi equation [13]), there are many approaches to calculate it. Here we use the momentum-space Feynman diagram technique. For simplicity, our calculation is done in the light-cone gauge, although one is free to work entirely in covariant gauge.

Evolution of the helicity-independent and helicity-dependent distributions are different, hence we treat the two cases separately.

#### A. Evolution of Parton-Helicity-Independent Distributions

In this subsection, we consider evolution of helicity-independent off-forward parton distributions. We use a generic notation  $E_{S,NS}(x; \xi; Q^2)$  to denote singlet and non-singlet quark density,

$$E_{S,NS}(x; \xi; Q^2) = \frac{1}{2} \int_0^1 \frac{d^Z}{2} e^{i x h P^0_j} \left( \frac{-n}{2} \right) \mathbb{P} i; \quad (13)$$

where the flavor indices have been ignored, and  $E_G(x; \xi; Q^2)$  to denote gluon distribution,

$$E_G(x; \xi; Q^2) = \frac{1}{x} \int_0^1 \frac{d^Z}{2} e^{i x h P^0_j} \mathbb{F} \left( \frac{-n}{2} \right) \mathbb{F} \left( \frac{-n}{2} \right) \mathbb{P} i n n : \quad (14)$$

The support for light-cone variables  $x$  and  $\xi$  can be studied as in Ref. [14] and is  $1 < x < 1$  and  $0 < \xi < 1$ , respectively. Since the evolution equations are independent of  $Q^2$ , we will omit the variable in the following equations.

The evolution of the non-singlet quark density at  $x > \xi=2$  takes the form,

$$\frac{dE_{NS}(x; \xi; Q^2)}{d \ln Q^2} = \frac{s}{2} \int_x^1 \frac{dy}{y} P_{NS} \left( \frac{x}{y}; - \right) E_{NS}(y; \xi; Q^2); \quad (15)$$

where the parton splitting function is calculated according to Fig. 3 (a). The result is,

$$P_{NS}(x; \xi) = C_F \frac{x^2 + 1 - \xi^2}{(1-x)(1-\xi^2)}; \quad (16)$$

where  $C_F = 4/3$  for SU(3) color group. Obviously, when  $\xi = 0$ , the splitting function becomes the usual Altarelli-Parisi evolution kernel. For  $\xi=2 < x < \xi=2$ , the evolution takes the form,

$$\frac{dE_{NS}(x; \xi; Q^2)}{d \ln Q^2} = \frac{s}{2} \int_x^1 \frac{dy}{y} P_{NS}^0 \left( \frac{x}{y}; - \right) \int_1^x \frac{dy}{y} P_{NS}^0 \left( \frac{x}{y}; - \right) E_{NS}(y; \xi; Q^2); \quad (17)$$

where

$$P_{NS}^0 = C_F \frac{x + \xi^2}{(1 + \xi^2) \left( 1 + \frac{\xi^2}{x} \right)}; \quad (18)$$

When  $\alpha_s = 1$ , after a suitable change of variables, the evolution equation becomes the Brodsky-Lepage evolution equation for the pion wavefunction [15]. For  $x < R_x = 2$ , the evolution takes the same form as Eq. (15), apart from the replacement  $R_1 \rightarrow R_x$ .

The evolution of the singlet-quark density mixes with that of the gluon density. For  $x > 2$ , the coupled evolution takes the form,

$$\begin{aligned} \frac{dE_S(x; ; Q^2)}{d \ln Q^2} &= \frac{s}{2} \int_x^1 \frac{dy}{Y} P_{SS} \left( \frac{x}{Y}; - \right) E_S(y; ; Q^2) + n_F P_{SG} \left( \frac{x}{Y}; - \right) E_G(y; ; Q^2) ; \\ \frac{dE_G(x; ; Q^2)}{d \ln Q^2} &= \frac{s}{2} \int_x^1 \frac{dy}{Y} P_{GS} \left( \frac{x}{Y}; - \right) E_S(y; ; Q^2) + P_{GG} \left( \frac{x}{Y}; - \right) E_G(y; ; Q^2) ; \end{aligned} \quad (19)$$

where  $n_F$  is the number of quark flavors. The evolution kernels are,

$$\begin{aligned} P_{SS}(x; ) &= P_{NS}(x; ) ; \\ P_{SG}(x; ) &= T_F \frac{x^2 + (1-x)^2}{(1-x^2)^2} ; \\ P_{GS}(x; ) &= C_F \frac{1 + (1-x)^2}{x(1-x^2)} ; \\ P_{GG}(x; ) &= C_A \frac{(x^2 - 2)}{x(1-x^2)^2} \left[ 1 + \frac{2(1-x)(1+x^2)}{x^2 - 2} + \frac{1+x}{1-x} \right] ; \end{aligned} \quad (20)$$

where  $T_F = 1/2$  and  $C_A = 3$ . As  $\alpha_s \rightarrow 0$ , we again get the usual Altarelli-Parisi evolution kernel.

For  $2 < x < 2$ , we have

$$\begin{aligned} \frac{dE_S(x; ; Q^2)}{d \ln Q^2} &= \frac{s}{2} \int_x^1 \frac{dy}{Y} P_{SS}^0 \left( \frac{x}{Y}; - \right) E_S(y; ; Q^2) \\ &+ \frac{s}{2} \int_x^1 \frac{dy}{Y} P_{SG}^0 \left( \frac{x}{Y}; - \right) E_G(y; ; Q^2) ; \\ \frac{dE_G(x; ; Q^2)}{d \ln Q^2} &= \frac{s}{2} \int_x^1 \frac{dy}{Y} P_{GS}^0 \left( \frac{x}{Y}; - \right) E_S(y; ; Q^2) \\ &+ \frac{s}{2} \int_x^1 \frac{dy}{Y} P_{GG}^0 \left( \frac{x}{Y}; - \right) E_G(y; ; Q^2) ; \end{aligned} \quad (21)$$

where the evolution kernels are,

$$\begin{aligned} P_{SS}^0(x; ) &= P_{NS}^0(x; ) ; \\ P_{SG}^0(x; ) &= T_F \frac{(x+2)(1-2x)}{(1+2)(1-x^2)} ; \\ P_{GS}^0(x; ) &= C_F \frac{(x+2)(2-x)}{x(1+2)} ; \\ P_{GG}^0(x; ) &= \frac{1}{2} C_A \frac{(x^2 - 2)}{x(1+2)(1-x^2)} \left[ 1 - \frac{(1+x)}{1-x} - \frac{4(1+x^2)}{x-2} \right] ; \end{aligned} \quad (22)$$

For  $x < 2$ , the evolution equations are the same as Eq. (19), except  $R_1 \rightarrow R_x$ .

B. Evolution of Parton-Helicity-Dependent Distributions

The helicity-dependent distributions are defined as follows: The singlet and non-singlet quark distributions are

$$\tilde{E}_{S,NS}(x; \lambda; Q^2) = \frac{1}{2} \int_0^1 dy e^{i\lambda y} hP^0_j \left( \frac{x}{2} \right) F_{S,NS} \left( \frac{x}{2}, y; Q^2 \right) \quad (23)$$

The gluon distribution is,

$$\tilde{E}_G(x; \lambda; Q^2) = \frac{i}{x} \int_0^1 dy e^{i\lambda y} hP^0_j F_G \left( \frac{x}{2}, y; Q^2 \right) \quad (24)$$

where  $F^{\lambda} = \frac{1}{2} F^{\lambda}$ .

The evolution of the non-singlet helicity-dependent quark density is exactly the same as that of the non-singlet helicity-independent quark density.

For the singlet evolution, we consider mixing between the singlet quark and gluon distributions. For  $x > 1/2$ , the evolution equations are,

$$\begin{aligned} \frac{d\tilde{E}_S(x; \lambda; Q^2)}{d \ln Q^2} &= \frac{s}{2} \int_0^1 \frac{dy}{x y} P_{SS} \left( \frac{x}{y}; - \right) \tilde{E}_S(y; \lambda; Q^2) + n_F P_{SG} \left( \frac{x}{y}; - \right) \tilde{E}_G(y; \lambda; Q^2); \\ \frac{d\tilde{E}_G(x; \lambda; Q^2)}{d \ln Q^2} &= \frac{s}{2} \int_0^1 \frac{dy}{x y} P_{GS} \left( \frac{x}{y}; - \right) \tilde{E}_S(y; \lambda; Q^2) + P_{GG} \left( \frac{x}{y}; - \right) \tilde{E}_G(y; \lambda; Q^2); \end{aligned} \quad (25)$$

where the splitting functions are,

$$\begin{aligned} P_{SS}(x; \lambda) &= P_{NS}(x; \lambda); \\ P_{SG}(x; \lambda) &= T_F \frac{x^2 (1-x)^2}{(1-x^2)^2}; \\ P_{GS}(x; \lambda) &= C_F \frac{1 - (1-x)^2}{x(1-x^2)}; \\ P_{GG}(x; \lambda) &= C_A \frac{(x^2 - 1)^2}{x(1-x^2)^2} \left( 1 + \frac{4x(1-x)}{x^2 - 1} + \frac{1+x}{1-x} \right); \end{aligned} \quad (26)$$

Again, when  $\lambda = 0$ , the splitting functions are the usual spin-dependent Altarelli-Parisi kernel. For  $1/2 < x < 1$ , the evolution equations are,

$$\begin{aligned} \frac{d\tilde{E}_S(x; \lambda; Q^2)}{d \ln Q^2} &= \frac{s}{2} \int_0^1 \frac{dy}{x y} P_{SS}^0 \left( \frac{x}{y}; - \right) \int_0^1 \frac{dy}{y} P_{SS}^0 \left( \frac{x}{y}; - \right) \tilde{E}_S(y; \lambda; Q^2) \\ &\quad + \frac{s}{2} \int_0^1 \frac{dy}{x y} P_{SG}^0 \left( \frac{x}{y}; - \right) \int_0^1 \frac{dy}{y} P_{SG}^0 \left( \frac{x}{y}; - \right) \tilde{E}_G(y; \lambda; Q^2); \\ \frac{d\tilde{E}_G(x; \lambda; Q^2)}{d \ln Q^2} &= \frac{s}{2} \int_0^1 \frac{dy}{x y} P_{GS}^0 \left( \frac{x}{y}; - \right) \int_0^1 \frac{dy}{y} P_{GS}^0 \left( \frac{x}{y}; - \right) \tilde{E}_S(y; \lambda; Q^2) \\ &\quad + \frac{s}{2} \int_0^1 \frac{dy}{x y} P_{GG}^0 \left( \frac{x}{y}; - \right) \int_0^1 \frac{dy}{y} P_{GG}^0 \left( \frac{x}{y}; - \right) \tilde{E}_G(y; \lambda; Q^2); \end{aligned} \quad (27)$$

where the splitting functions are,

$$\begin{aligned}
P_{SS}^0(x; \epsilon) &= P_{NS}^0(x; \epsilon); \\
P_{SG}^0(x; \epsilon) &= T_F \frac{(x + \epsilon = 2)(1 + \epsilon = 2)}{(1 + \epsilon = 2)(1 - \epsilon = 2)}; \\
P_{GS}^0(x; \epsilon) &= C_F \frac{(x + \epsilon = 2)^2}{x(1 + \epsilon = 2)}; \\
P_{GG}^0(x; \epsilon) &= \frac{1}{2} C_A \frac{(x^2 - \epsilon = 2)}{x(1 - \epsilon = 2)(1 - \epsilon = 2)} - 1 - \epsilon = 2 \frac{(1 + x + \epsilon)}{1 - x} - \frac{8x}{x - \epsilon = 2} : \quad (28)
\end{aligned}$$

Of course, in a reasonable range of  $Q^2$ , the OCFDs do not evolve dramatically. Thus, a second check on the DVCS dynamical mechanism is to find small  $Q^2$  dependences of relevant scaling functions.

#### IV. CROSS SECTIONS AND ESTIMATES

In this section, we calculate the cross section for electroproduction of a real photon on a nucleon. As shown in Fig. 4, we use  $k = (k^0; \vec{k})$  and  $k^0 = (k^0; \vec{k}^0)$  to denote the four-momenta of the initial and final electron,  $P = (M; \vec{0})$  and  $P^0 = (E^0; \vec{P}^0)$  the initial and final momenta of the nucleon,  $q^0 = (q^0; \vec{q}^0)$  the momentum of the final photon. The differential cross section in the laboratory frame is,

$$d = \frac{1}{4!M} \mathcal{T} \int \int (2)^4 (k + P - k^0 - P^0 - q^0) \frac{d^3 \vec{k}^0}{2!^0(2)^3} \frac{d^3 \vec{P}^0}{2E^0(2)^3} \frac{d^3 \vec{q}^0}{2^0(2)^3}; \quad (29)$$

where  $M$  is the nucleon mass and  $\mathcal{T}$  is the T-matrix of the scattering. Integrating over the photon momentum, we find,

$$d = \frac{1}{4!M} \mathcal{T} \int \int \frac{!^0 d^0 d}{2(2)^3} 2 \left( (k + P - k^0 - P^0)^2 \right) \frac{d^3 \vec{P}^0}{2E^0(2)^3}; \quad (30)$$

where  $\delta$ -function reflecting the photon on-shell condition, which imposes a relation between the direction and magnitude of the momentum of the recoiling nucleon,  $P^0$ ,

$$s + M^2 - 2((k + M)E^0 - \vec{q} \cdot \vec{P}^0) = 0 \quad (31)$$

where  $s = (q + P)^2$ ,  $q = (q^0; \vec{q}) = k - k^0$ . Thus the phase space of the recoiling proton is specified by the solid angle  $d_P^0$ . Note, however, that for large  $s$  and  $\epsilon$ , there are two solutions of  $\vec{P}^0$  corresponding to one orientation of  $P^0$ . Physically one of them represents the recoil proton at the backward angle in the center-of-mass frame. Integrating over the magnitude of  $P^0$ , we get,

$$d = \frac{1}{32(2)^5!M} !^0 d^0 d_{e^0 d_P^0} \frac{P^0}{\vec{P}^0 \cdot (k + M) - qE^0 \cos \theta_j} \mathcal{T} \int \int; \quad (32)$$

where  $\theta_j$  is the angle between  $\vec{q}$  and  $\vec{P}^0$ , and the sum over two possible solutions of  $\vec{P}^0$  is implicit. We choose the z-axis to be the direction of the incident electron and the x-axis in

the plane formed by the initial and final electron momenta. In this coordinate system, the final electron has the polar angle  $\theta$ . The polar and azimuthal angles of  $\mathbf{P}^0$  are denoted by  $\theta_P^0$  and  $\phi_P^0$ , respectively. Note that  $\int d^3j$  has the dimension of a cross section.

Alternatively, we can integrate out the momentum of the recoil proton,

$$d^3j = \frac{1}{32(2\pi)^5 M} \int d^3d \int d^3e \int d^3q \frac{1}{j^2 + M^2} \frac{1}{q \cos \theta_j^0} \int d^3j^0; \quad (33)$$

where  $\theta^0$  is the angle between  $\mathbf{q}$  and  $\mathbf{q}^0$ . The polar and azimuthal angles of  $\mathbf{q}^0$  are denoted by  $\theta_q^0$  and  $\phi_q^0$ , respectively. The constraint between the energy and direction of the outgoing photon is,

$$s - M^2 - 2^0( + M - q \cos \theta^0) = 0; \quad (34)$$

#### A. T-matrix

We calculate the Feynman diagrams shown in Fig. 4. We assume for the moment that the scattering lepton is negatively charged. The T-matrix for the Compton scattering part is,

$$T_1 = e^3 u(k^0) \bar{u}(k) \frac{1}{q^2} T; \quad (35)$$

where  $u; \bar{u}$  are the spinors of the lepton and  $\epsilon$  is the polarization of final photon.  $T$  is the standard Compton amplitude,

$$T = i \int d^4z e^{iqz} \bar{h} P^0 \bar{J}(z) J(0) \mathcal{P} i d^4z; \quad (36)$$

In the deep-virtual region,  $T$  is expressed in terms of off-forward parton distributions in Eq. (4).

The T-matrix for the Bethe-Heitler (BH) process is,

$$T_2 = e^3 u(k^0) \bar{u}(k) = \frac{1}{\not{k} - m_e + i} + \frac{1}{\not{k}^0 + m_e + i} = \bar{u}(k) \frac{1}{2} \bar{h} P^0 \bar{J}(0) \mathcal{P} i; \quad (37)$$

where  $m_e$  is the mass of electron and will be ignored for the following discussion. The elastic nucleon matrix element is,

$$\bar{h} P^0 \bar{J}(0) \mathcal{P} i = U(P^0) [F_1(\tau^2) + F_2(\tau^2) \frac{i \not{q}}{2M}] U(P); \quad (38)$$

where  $U; \bar{U}$  are the nucleon spinors and  $F_1$  and  $F_2$  are the usual Dirac and Pauli form factors of the nucleon.

The total T-matrix is the sum of the two above,

$$T = T_1 + T_2; \quad (39)$$

## B. Unpolarized Scattering

First, we consider the scattering process without polarizations. The square of the T-matrix has three terms. First, the pure Compton process gives,

$$\mathbb{T}_1^2 = \frac{e^6}{q^4} v_{VC} W_{VC} ; \quad (40)$$

where the lepton tensor is,

$$v_{VC}^{(\cdot)} = 2(k^0 k^0 + k^0 k^0 - g_{\mu\nu} k^\mu k^\nu) ; \quad (41)$$

The hadron tensor is calculated from Eq. (4),

$$\begin{aligned} W_{VC}^{(\cdot)} = & \frac{1}{4} (g_{\mu\nu} p^\mu n^\nu - p^\mu p^\nu) \int dx^0(x) \int dx^0(x^0) \\ & [ \int dx^0(x) \int dx^0(x^0) (H^2(x; ;^2) + E^2(x; ;^2)) (H^2(x^0; ;^2) + E^2(x^0; ;^2)) \\ & + 4H(x; ;^2)H(x^0; ;^2) - \frac{2}{M^2} E^2(x; ;^2)E^2(x^0; ;^2) ] \\ & + \int dx^0(x) \int dx^0(x^0) [ \int dx^0(x) \int dx^0(x^0) (H^2(x; ;^2) + E^2(x; ;^2)) (H^2(x^0; ;^2) + E^2(x^0; ;^2)) \\ & + 4H^2(x; ;^2)H^2(x^0; ;^2) + 2E^2(x; ;^2)E^2(x^0; ;^2) (1 - \frac{2}{4M^2}) ] ; \end{aligned} \quad (42)$$

where  $\tilde{x}(x)$  and  $\tilde{x}(x)$  are,

$$\begin{aligned} \tilde{x}(x) &= \frac{1}{x - 2 + i} + \frac{1}{x + 2 - i} ; \\ \tilde{x}(x) &= \frac{1}{x - 2 + i} - \frac{1}{x + 2 - i} ; \end{aligned} \quad (43)$$

Thus, for  $H(x)$  and  $E(x)$  less singular than  $x^{-2}$  and  $H^*(x)$  and  $E^*(x)$  less singular than  $x^{-1}$ , the integrals are convergent. To simplify the expression, we have left out as usual the sum over quark flavors weighted by the electric charge squared. To find the product of the two tensors, one shall express the null-vectors  $n$  and  $p$  in terms of physical vectors  $P$  and  $q$  by inverting Eq. (3). The result is that  $\mathbb{T}_1^2$  goes like  $1=Q^2$  at large  $Q^2$ , like the inclusive deep-inelastic process.

The pure Bethe-Heitler process gives,

$$\mathbb{T}_2^2 = \frac{e^6}{4} v_{BH}^{(\cdot)} W_{BH}(\cdot) ; \quad (44)$$

where the lepton tensor is

$$\begin{aligned} v_{BH}^{(\cdot)} = & \frac{8}{(k^0 + k^0)^4} [k^\mu (k^\mu + k^0)] (2k^0 k^0 + k^0 k^0 + k^0 k^0 - g_{\mu\nu} k^\mu k^\nu) \\ & + \frac{8}{(k^0)^4} [k^\mu (k^\mu)] (2k^\mu k^\mu - k^\mu k^\mu + g_{\mu\nu} k^\mu k^\nu) \\ & + \frac{8}{(k^0)^2 (k^0 + k^0)^2} [2(k^0 + k^0) (k^\mu k^\mu + k^0 k^0) + 2(k^0 k^0 - k^\mu k^\mu) \\ & + (k^\mu k^\mu + k^0 k^0) + (k^\mu k^\mu) + (k^\mu k^\mu) + (k^0 k^0) - g_{\mu\nu} k^\mu k^\nu] ; \end{aligned} \quad (45)$$

As  $Q^2 \rightarrow 0$ , it diverges quadratically as expected from low-energy theorems. The hadron tensor is,

$$W_{BH}^{(\mu\nu)} = (F_1(Q^2) + F_2(Q^2))^2 (2g^{\mu\nu} + (P + \frac{Q}{2})^\mu (P + \frac{Q}{2})^\nu - 4(F_1(Q^2))^2 - \frac{2}{4M^2} F_2(Q^2)^2); \quad (46)$$

which is well-known from elastic scattering. Although the product of the two tensors is complicated in general, it simplifies to

$$\mathbb{T}_2^{\mu\nu} = \frac{8e^6 M^2 Q^2}{4} \frac{1}{k^\mu} \frac{1}{k^\nu} : \quad (47)$$

as  $Q^2 \rightarrow 0$ . Thus, for small  $Q^2$ , the cross section of the Bethe-Heitler process dominates that of DVCS. To have a clear DVCS signal, one must have a  $Q^2$  reasonably large (at least on the order of the nucleon mass) and not a too large  $Q^2$ .

To appreciate the relative and absolute sizes of the DVCS and BH cross sections, we shown in Fig. 5 some calculations at the electron beam energies  $E = 6$  GeV (CEBAF after upgrading) and  $E = 30$  GeV (DESY). For the Bethe-Heitler process, the cross section can be evaluated accurately using the experimentally-measured nucleon form factors. For the DVCS cross section, we need a model for the OFPDs. Since we are interested in only a rough estimate, we keep only the  $H^2$  terms in Eq. (42) and assume,

$$H(x; Q^2) = q(x)e^{-x^2} : \quad (48)$$

In Fig. 5a, we have shown the DVCS (solid) and BH (dashed) cross sections at incident electron energy  $E = 6$  GeV and scattering angle  $\theta = 15^\circ$ , with a virtual photon  $E_\gamma = 3$  GeV and  $Q^2 = 1.2$  GeV<sup>2</sup>. The recoil proton is detected in the electron scattering plane and at the same side of the scattered electron. The result shows that when  $Q^2 > 1$  GeV<sup>2</sup>, the DVCS cross section dominates the BH cross section. In Fig. 5b, we have shown similarly cross sections at  $E = 30$  GeV and scattering angle  $\theta = 7^\circ$ , with the photon energy  $E_\gamma = 15$  GeV,  $Q^2 = 6.7$  GeV<sup>2</sup>. Here the BH cross section dominates till large recoils. Since the BH cross section is calculable, the DVCS amplitude can be extracted potentially from the interference cross section which we now turn to.

The interference contribution has the following structure,

$$T_1 T_2 + T_1 T_2 = 2 \frac{e^6}{2Q^2} \text{Re} H^{(\mu\nu)} + \text{Re} H^{[\mu\nu]} : \quad (49)$$

where the lepton tensor has been divided into symmetric and antisymmetric parts according to the indices  $\mu$  and  $\nu$ . The symmetric lepton tensor is

$$\begin{aligned} \text{Re} H^{(\mu\nu)} = & \frac{2}{(k^0)^2} \left[ (k^0 k^\mu + k^0 k^\nu) (k^\mu k^\nu) + [k^0 (k^\mu k^\nu) + k^0 (k^\nu k^\mu)] k^\mu \right. \\ & \left. + (k^0 g^{\mu\nu} + k^0 g^{\nu\mu}) (k^\mu k^\nu) \right. \\ & \left. + g^{\mu\nu} [k^\mu k^\nu + k^\nu k^\mu] + k^0 (k^\mu k^\nu) + k^0 (k^\nu k^\mu) \right] \\ & + \frac{2}{(k^0)^2} \left[ (k^0 k^\mu + k^0 k^\nu) (k^0 k^\mu + k^0 k^\nu) + [k^\mu (k^0 k^\nu) + k^\nu (k^0 k^\mu)] k^0 \right. \\ & \left. + (k^\mu g^{\nu\mu} + k^\nu g^{\mu\nu}) (k^0 k^\mu + k^0 k^\nu) \right. \\ & \left. + g^{\mu\nu} [k^\mu (k^0 k^\nu) + k^\nu (k^0 k^\mu)] + k^\mu (k^\nu k^0) + k^\nu (k^\mu k^0) \right] ; \quad (50) \end{aligned}$$

and the antisymmetric lepton tensor is

$$\begin{aligned} v^{[ij]} = & \frac{2}{(k^0)^2} k^i k^j (g^{00} - g^{ij}) + k^0 (k^i g^{0j} - k^j g^{0i}) \\ & + k^0 (k^i g^{0j} - k^j g^{0i}) - k^i (k^0 g^{0j} - k^j g^{00}) : \end{aligned} \quad (51)$$

As  $\epsilon \rightarrow 0$ , the symmetric part dominates over the antisymmetric part.

The hadron tensor is also separated into two contributions. The symmetric part is,

$$\begin{aligned} H^{(ij)} = & \int d^4x (g^{ij} - p^i p^j) \langle \dots \rangle \\ & (F_1(\epsilon^2) + F_2(\epsilon^2)) (E(x; \epsilon^2) + H(x; \epsilon^2)) \left[ \frac{1}{2} + \frac{1}{2} n^i \right] \\ & + 2P^i [H(x; \epsilon^2) F_1(\epsilon^2) - \frac{1}{4M^2} E(x; \epsilon^2) F_2(\epsilon^2)] n^i ; \end{aligned} \quad (52)$$

and the antisymmetric part is

$$H^{[ij]} = \int d^4x (x^i p^j - x^j p^i) (F_1(\epsilon^2) + F_2(\epsilon^2)) H^i(x; \epsilon^2) : \quad (53)$$

The final expression for products of the tensors above is quite lengthy and is omitted. It is generally believed that the interference contribution has a size between the BH and DVCS cross sections. Thus, if the BH cross section is much larger than that of DVCS, the DVCS amplitude might be accessible through the interference term which, for instance, can be extracted by comparing the electron and positron scattering, or by direct subtraction.

### C. Double Spin Process

In this subsection, we consider scattering with both the lepton beam and nucleon target polarized. The structure of the cross section is similar to the unpolarized case. Indeed, the spin-dependent part of the T-matrix squared has three contributions. The pure virtual Compton process gives,

$$\mathcal{T}_{1j}^2 = \frac{e^6}{Q^4} v_{VC}^{[ij]} W_{VC}^{[ij]} : \quad (54)$$

The spin-dependent lepton tensor is antisymmetric,

$$v_{VC}^{[ij]} = 2i \epsilon^{ijk} k^0 ; \quad (55)$$

where  $\epsilon = \pm 1$  represent the positive or negative helicity of the scattering lepton. The spin-dependent hadron tensor is also antisymmetric,

$$\begin{aligned}
W_{VC}^{[1]} = & \frac{i}{2} \int_{p_n}^z \int_{dx}^z dx^0 \text{Re}[(x)(x^0)]^h 4H(x; ;^2)H(x^0; ;^2)(S_n)(1 - \frac{1}{2}) \\
& 2E(x; ;^2)H(x^0; ;^2)[(S_n)(\frac{2}{2M^2}) - \frac{(S_n)}{M^2}(1 + \frac{1}{2})] \\
& + (H(x; ;^2) + E(x; ;^2))E(x^0; ;^2)\frac{1}{M^2}[(S_n)(1 + \frac{1}{2}) + (S_n)\frac{2}{2}] \\
& + E(x; ;^2)E(x^0; ;^2)\frac{1}{M^2}(S_n) : \quad (56)
\end{aligned}$$

Using  $\epsilon_{\mu\nu\alpha\beta} = 2(g_\mu\alpha g_\nu\beta - g_\mu\beta g_\nu\alpha)$ , one can straightforwardly work out the product of the two tensors.

The pure Bethe-Heitler process gives,

$$T_2^j = \frac{e^6}{4} v_{BH}^{[1]} W_{BH}^{[1]} : \quad (57)$$

The antisymmetric lepton tensor is

$$\begin{aligned}
v_{BH}^{[1]} = & \frac{8i}{\#} \left[ \frac{k^0(k^0 + )}{(k^0 + )^4} + \frac{k(k - )}{(k - )^4} - \frac{k^0}{(k - )^2(k^0 + )^2} \right] ; \quad (58)
\end{aligned}$$

and the antisymmetric hadron tensor is,

$$\begin{aligned}
W_{BH}^{[1]} = & i \int_{2(F_1(-^2) + F_2(-^2))}^h (F_1(-^2) + \frac{2}{4M^2}F_2(-^2)) S \\
& + F_2(-^2)(F_1(-^2) + F_2(-^2))\frac{(S)}{M^2} P^i : \quad (59)
\end{aligned}$$

As  $\epsilon \rightarrow 0$ , the lepton tensor is subleading relative to the spin-independent counterpart shown in Eq. (45). Thus the spin asymmetry in the BH process vanishes in such a limit.

Finally, we consider the interference contribution,

$$T_1 T_2 + T_1 T_2 = 2 \frac{e^6}{2Q^2} v^{(\cdot)} \text{Re}[H^{(\cdot)}] + v^{[1]} \text{Re}[H^{[1]}] ; \quad (60)$$

where the spin-dependent lepton tensor has both symmetric and antisymmetric parts. The symmetric part is,

$$\begin{aligned}
v^{(\cdot)} = & \frac{2i}{(k - )^2} k^0 + k^0 g k^0 k \\
& + \frac{2i}{(k^0 + )^2} k + k g k k^0 ; \quad (61)
\end{aligned}$$

and the antisymmetric part is

$$\begin{aligned}
v^{[1]} = & \frac{2}{(k - )^2} i (k - ) k + k (k - ) + g k k^0 \\
& \frac{2}{(k^0 + )^2} i (k^0 + ) k^0 + k^0 (k^0 + ) g k^0 k : \quad (62)
\end{aligned}$$

As  $\epsilon \rightarrow 0$ , the antisymmetric part dominates over the symmetric part.

The spin-dependent hadron tensor is separated into two parts accordingly. The symmetric part is,

$$\begin{aligned}
 H^{(S)} = & \int_0^1 dx \langle x | \left( (F_1(x^2) + F_2(x^2)) (E(x; \epsilon^2) + H(x; \epsilon^2)) \right. \\
 & \left. + F_2(x^2) (H(x; \epsilon^2) + E(x; \epsilon^2)) \frac{P \cdot S}{M^2} \right. \\
 & \left. + (F_1(x^2) + F_2(x^2)) E(x; \epsilon^2) \frac{1}{M^2} P \cdot S \right) | \epsilon \rangle
 \end{aligned} \quad (63)$$

and the antisymmetric part is,

$$\begin{aligned}
 H^{(A)} = & \int_0^1 dx \langle x | \left( (F_1(x^2) + F_2(x^2)) H(x; \epsilon^2) (S \cdot n) \mathcal{P} \cdot S \right. \\
 & \left. + 2H(x; \epsilon^2) F_2(x^2) \mathcal{P} \cdot (S \cdot n) \left( 1 - \frac{2}{4M^2} \right) \frac{(S \cdot n)}{2M^2} \left( 1 + \frac{1}{2} \right) \right. \\
 & \left. + (F_1(x^2) + F_2(x^2)) E(x; \epsilon^2) \frac{1}{2M^2} \left[ (S \cdot n) \mathcal{P} + \frac{2}{2} S \cdot n \right] \right. \\
 & \left. + \frac{1}{2M^2} F_2(x^2) E(x; \epsilon^2) (S \cdot n) \mathcal{P} \cdot S \right) | \epsilon \rangle
 \end{aligned} \quad (64)$$

The product of tensors leads to a lengthy expression which we omit.

#### D. Single-Spin Process

The virtual Compton amplitude is complex because of the intermediate quark propagation. This gives rise to the so-called single-spin asymmetry, that is, the cross-section asymmetry depending on a single polarization. For instance, suppose the lepton beam is polarized and the hadron is unpolarized, the single-spin asymmetry is proportional to

$$A_{LT}^e = 2 \frac{e^6}{2Q^2} \langle \epsilon \rangle \text{Im} H^{(S)} + \langle \epsilon \rangle \text{Im} H^{(A)} : \quad (65)$$

On the other hand, if the nucleon is polarized and the lepton is unpolarized, the single-spin asymmetry is proportional to

$$A_{LT}^N = 2 \frac{e^6}{2Q^2} \langle \epsilon \rangle \text{Im} [H^{(S)}] + \langle \epsilon \rangle \text{Im} [H^{(A)}] : \quad (66)$$

The size of these spin asymmetries directly reflect the relative contributions of the DVCS and BH processes. Their measurement and interpretation are very interesting although they only depend on the parton distributions at  $x = \epsilon = 2$ .

## V. COMMENTS AND CONCLUSIONS

In this paper, we studied some basic aspects of deeply-virtual Compton scattering. The motivation is that in the deeply-virtual kinematics, the scattering mechanism appears to be simple, and hence, one can learn some structural information from the process. The QCD analysis shows that it is the  $o$ -forward parton distributions that are probed. In a particular experiment, of course, one has to decide whether one is at the deeply-virtual kinematics. As we discussed in the paper, one can look at certain observables which vanish in the kinematic limit (like  $R = \sigma_L = \sigma_T$  in deep-inelastic scattering). Those include  $\sigma_L$ ,  $\sigma_{TT}$  and  $\sigma_{LT}$  discussed in Ref. [11]. One can also check the slow  $-Q^2$  dependence of certain scaling functions. As a first guess, one shall be at least at the deep-inelastic kinematic region, and the recoil nucleon shall be at backward angles. It would be interesting to demonstrate experimentally that the single-quark scattering mechanism is at work.

One important theoretical issue is whether a factorization theorem exists for the deeply-virtual Compton process. The answer is most likely yes for several reasons. First, the tree result we obtained can be easily cast into an operator product expansion. Such an expansion is generally believed to be valid independent of external states. Second, the radiative corrections to the tree process are quite similar to the corrections to  $\sigma_{\text{BH}}$ , a process known to be factorizable at one loop level. Nonetheless, one still has to prove explicitly the factorization theorem for DVCS, which will be done in a separate publication.

DVCS at small  $Q^2$  is especially interesting, because the nucleon form-factor suppression is small and because  $Q^2 \rightarrow 0$  limit is relevant to the spin structure of the nucleon. However, due to QED infrared divergence, the Bethe-Heitler process becomes dominant there despite the fact that the DVCS cross section scales like the deep-inelastic scattering cross section. Thus one cannot go to too small  $Q^2$ . One may get around this to some extent by isolating the DVCS and BH interference term through single-spin asymmetry and/or combined lepton-antilepton scattering. Theoretical study of  $Q^2$  dependence of the OFPDs, in particular, its relation to the meson-dominance and the exponential decay law for exclusive cross section, is urgently needed.

The OFPDs depend on four independent variables: the Bjorken-type of variable  $x$ , the Feynman variable  $x$ , the momentum transfer  $Q^2$  and the virtual-photon mass  $Q^2$ . It is unlikely that one can learn the entire parameter space of the distributions in one kind of experiments. As our formulas show, different kinds of experiments are sensitive to different combinations of parton distributions and hence they are complementary to each other. [The reason that the nucleon helicity- $ip$  distributions contribute to unpolarized scattering is similar to that the Pauli-form factor  $F_2(Q^2)$  appears in unpolarized elastic scattering.] However, to be able to study some rules, one must have accurate data in an extended kinematic region. To achieve this, one must have dedicated experiments at a suitable machine like EELFE for extended running [16].

The  $o$ -forward parton distributions can also be defined for quark helicity- $ip$  (chiral-odd) correlations and for higher twists. DVCS provides one process to access to these distributions. There are other processes one can consider to measure them. For instance, the diffractive  $\rho$  or  $J/\psi$  production studied by Brodsky et al. [17] can be used to measure the  $o$ -forward gluon distributions. Recently, Radyushkin has published a paper aimed at this direction [18]. Thus there is now a new territory to explore the quark and gluon structure

of the nucleon besides the traditional inclusive (parton distributions) and exclusive (form factors) processes.

#### A C K N O W L E D G M E N T S

I thank D . Beck, S . Brodsky, R . Jaffe, R . M cKeown, A . Nathan and A . Radyushkin for their discussions and interest, P . Guichon for his constructive comments about the manuscript, and O . Teryaev for pointing out reference [10].

## REFERENCES

- [1] A . H . Compton, *Phys. Rev.* 22 (1923) 409.
- [2] F . Low, *Phys. Rev.* 96 (1954) 1428; M . Gell-Mann and M . L . Goldberger, *Phys. Rev.* 96 (1954) 1433.
- [3] See for instance, V . B . Berestetskii, E . M . Lifshitz and L . P . Pitaevskii, *Quantum Electrodynamics*, Pergamon Press, 1980.
- [4] F . J . Federspiel et al., *Phys. Rev. Lett.* 67 (1991) 1511; A . Zieger et al., *Phys. Lett. B* 278 (1992) 34; E . Hallin et al., *Phys. Rev. C* 48 (1993) 1497.
- [5] G . R . Farrar, G . Sternan, and H . Zhang, *Phys. Rev. Lett.* 62 (1989) 2229; G . R . Farrar and H . Zhang, *Phys. Rev. D* 41 (1990) 3348.
- [6] S . J . Brodsky and G . R . Farrar, *Phys. Rev. Lett.* 31 (1973) 1153.
- [7] X . Ji, hep-ph/9603249, MIT-CTP-2517, March, 1996.
- [8] J . Ashman et al., *Nucl. Phys. B* 328 (1989) 1; B . Adeva et al., *Phys. Lett. B* 302 (1993); P . L . Anthony et al., *Phys. Rev. Lett.* 71 (1993) 959; K . Abe et al., *Phys. Rev. Lett.* 75 (1995) 25.
- [9] A . V . Radyushkin, *Phys. Lett. B* 380 (1996) 417.
- [10] F . M . Dittes, D . Muller, D . Robaschik, B . Geyer, and J . Horejsi, *Phys. Lett. B* 209 (1988) 325; B . Geyer, D . Robaschik, M . Bordag, and J . Horejsi, *Z. Phys. C* 26 (1985) 591; T . Braunshweig, B . Geyer, J . Horejsi, and D . Robaschik, *Z. Phys. C* 33 (1987) 275.
- [11] P . Kroll, M . Schumann, and P . A . M . Guichon, *Nucl. Phys. A* 598 (1996) 435.
- [12] R . L . Jaffe and X . Ji, *Phys. Rev. Lett.* 67 (1991) 552.
- [13] G . Altarelli and G . Parisi, *Nucl. Phys. B* 126 (1977) 278.
- [14] R . L . Jaffe, *Nucl. Phys. B* 229 (1983) 205.
- [15] G . P . Lepage and S . J . Brodsky, *Phys. Rev. D* 22 (1980) 2157;
- [16] J . Arvieux and E . de Sanctis, *The ELFE project*, Italian Physical Society Conference Proceeding 44 (1993).
- [17] S . J . Brodsky, L . Frankfurt, J . F . Gunion, A . H . Mueller, M . Strikman, *Phys. Rev. D* 50 (1994) 3134.
- [18] A . V . Radyushkin, hep-ph/9605431, CEBAF-TH-96-06, May, 1996.

## FIGURES

FIG .1. Virtual Compton scattering process.

FIG .2. QCD diagrams for deeply-virtual Compton scattering: a). the hand-bag diagram, b). & c). some  $1=Q^2$  corrections, d). & e). some radiative corrections.

FIG .3. Leading-log evolution of the  $0^-$ -forward parton distributions.

FIG .4. Electroproduction of a photon off the nucleon: a). the virtual Compton scattering, b). & c). the Bethe-Heitler process.

FIG .5. Comparison of the DVCS and BH cross sections at a). CEBAF and b). HERMES kinematics.

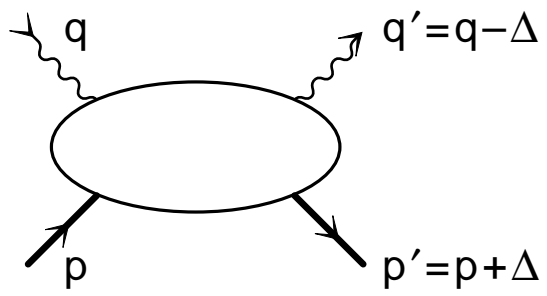
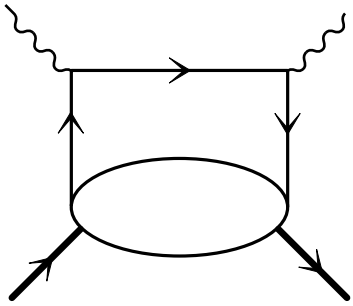
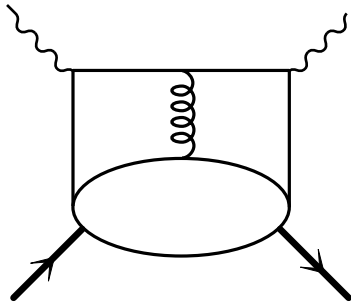


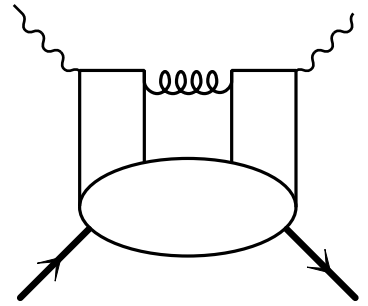
Fig. 1



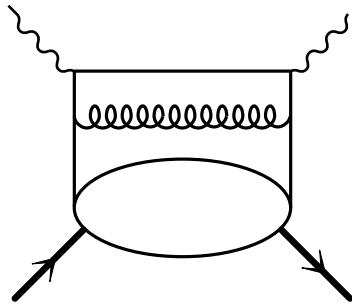
(a)



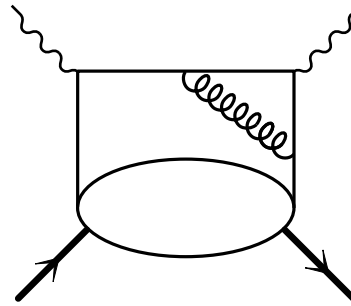
(b)



(c)

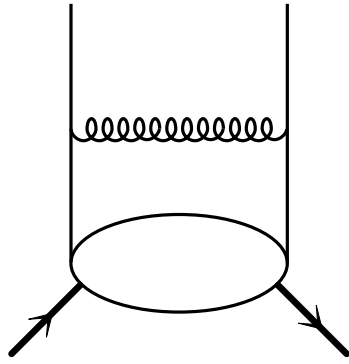


(d)

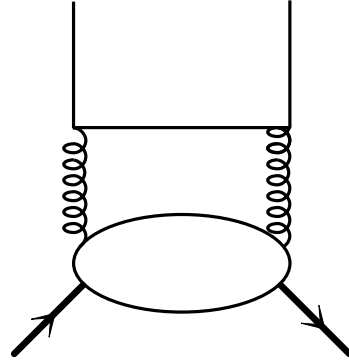


(e)

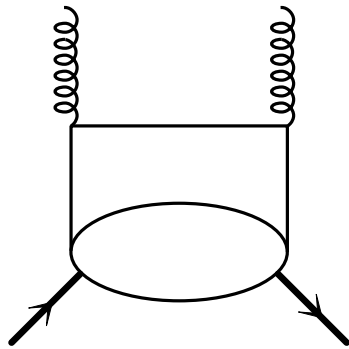
Fig. 2



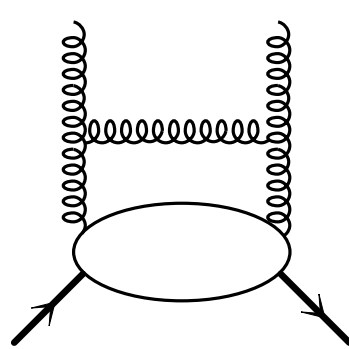
(a)



(b)

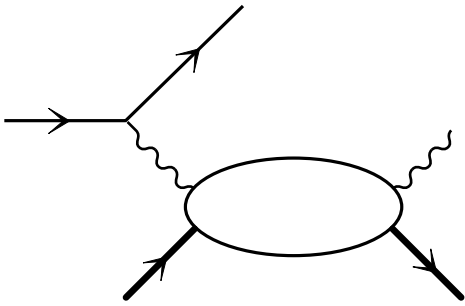


(c)

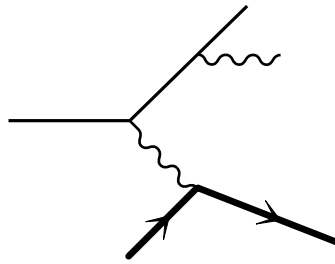


(d)

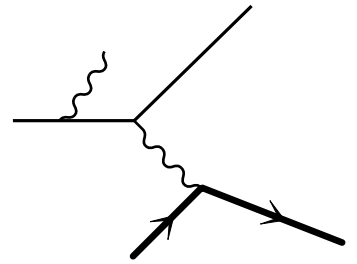
Fig. 3



(a)



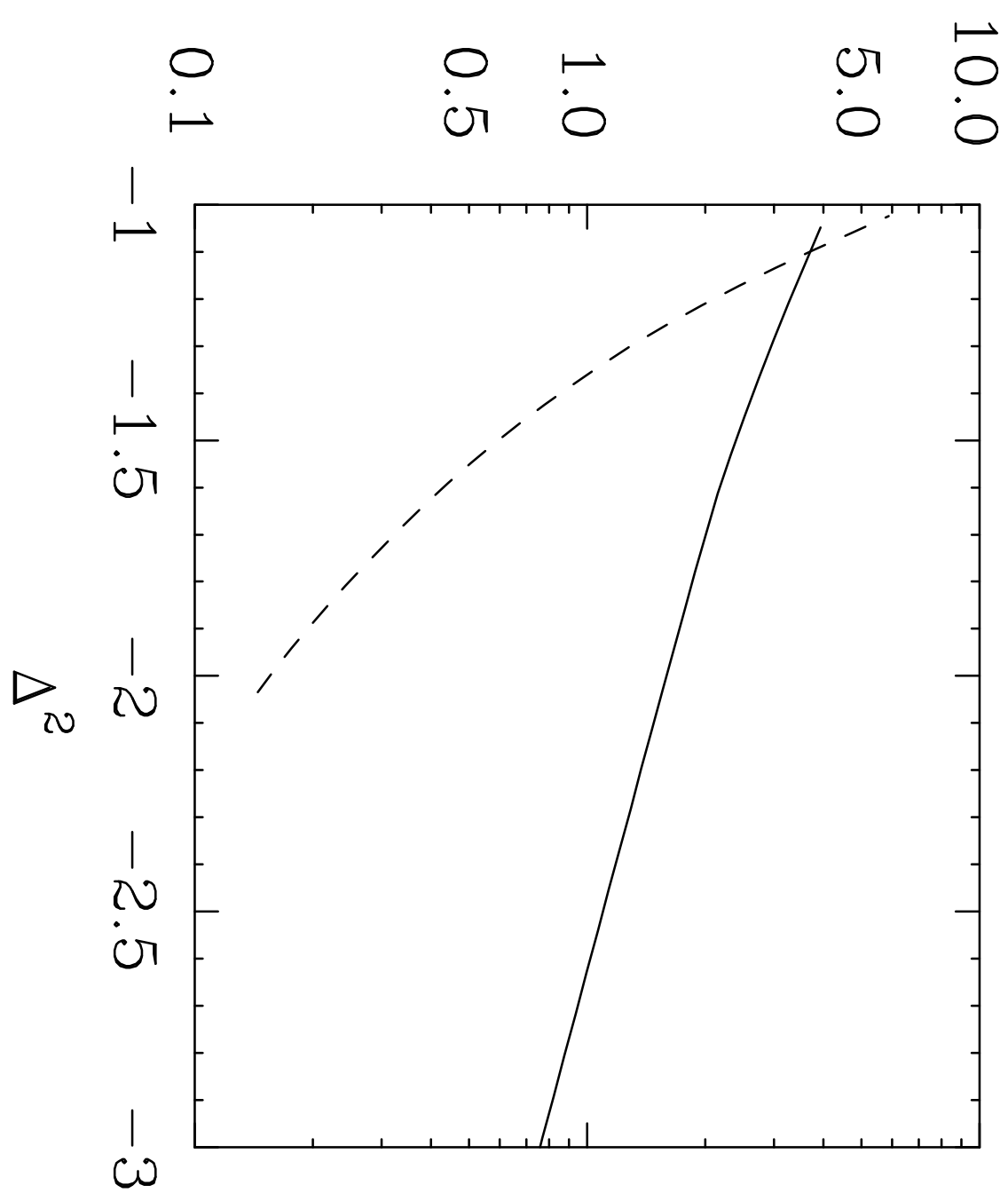
(b)



(c)

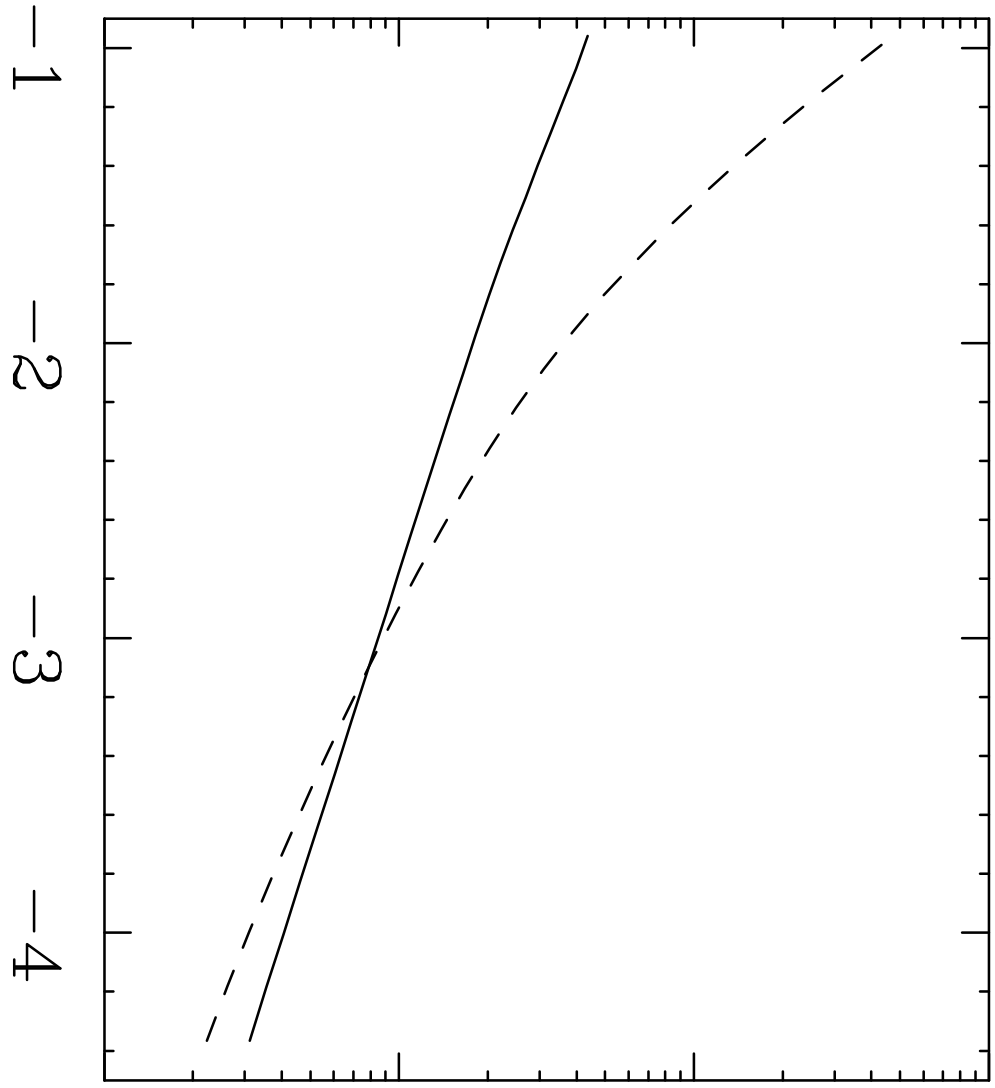
Fig. 4

$d^5\sigma/d\omega'd\Omega_e d\Omega_{P'}(\text{nb}/\text{GeV})$



$d^5\sigma/d\omega'd\Omega_e d\Omega_p$  (nb/GeV)

$10^1$   
 $10^0$   
 $10^{-1}$   
 $10^{-2}$



$\Delta^2$

-1  
-2  
-3  
-4